

Application of Additive Manufacturing Based Thermal Printing Techniques for Realization of Electronically Rewritable Chipless RFID Tags on Flexible Substrates

Jayakrishnan Methapettyparambu Purushothama⁽¹⁾, Sergio Lopez-Soriano⁽²⁾, Arnaud Vena⁽³⁾, Brice Sorli⁽³⁾, and Etienne Perret^(1,4)

(1) Université Grenoble Alpes, Grenoble INP, LCIS, 26000 Valence, France.

(2) Formerly with the Université Grenoble Alpes, Grenoble INP, LCIS, 26000 Valence, France, and now with the Department of Communications and Information Technology, Universitat Pompeu Fabra, Barcelona, Spain.

(3) Institut d'Electronique et des Systèmes, Université de Montpellier / CNRS, Montpellier 34095, France.

(4) Institut Universitaire de France, 75005 Paris, France.

Email: jayakrishnan.mp@lcis.grenoble-inp.fr, sergio.lopez@upf.edu, arnaud.vena@umontpellier.fr, brice.sorli@ies.univ-montp2.fr, etienne.perret@lcis.grenoble-inp.fr

Abstract

In this article, we present the design and realization of an electronically rewritable RF encoding particle (REP) for chipless RFID applications. This (REP) resonator geometry is integrated with two conductive bridging random access memory (CBRAM) based non-volatile RF switches, and could be electronically programmed using DC pulses to any of possible four resonant states to represent two bits of information. Emerging additive manufacturing (AM) technique based thermal transfer printing is utilized for the realization of this resonator on flexible and low cost Polyethylene terephthalate (PET) substrate. At present the size of the REP is such that five such REPs could be arranged on a standard credit card size tag. Also this REP encodes the most number of bits reported among non-volatile electronically rewritable REPs for chipless RFID applications – 2 bits, till date.

1 Introduction

Multi-scatter based chipless RFID is an emerging technology of smart identifiers [1]–[3]. Similar in appearance to the very well-known optical barcode identifiers, multi-scatterer based chipless RFID tags consist of some narrow band scatters (REPs) arranged on a suitable substrate. Data is encoded in these tags in form of the position of these narrowband resonances in a given frequency window [4]. The easiest and most commonly used techniques for the detection of such tags are through the measurement of its Radar Cross Section (RCS) response. These scatterers upon illuminated by an electromagnetic energy beam of a given bandwidth, re-scatter a unique pattern usually known as the RF-Signature of the tag. This data consists of the magnitude and phase information of the resonant characteristic of the REPs arranged on the tag. Several low cost RCS readers suitable for chipless RFID applications has been affirmatively reported till date [5], [6].

In contrast to optical barcode systems, chipless RFID tags are resistant to non-line of sight reading and could integrate several sensors among them and are thus suitable for application in areas like food safety, item

tracking, Internet of Things (IoT) and so on as a low cost smart identifier [1]–[3], [7].

One of a recent advance among the chipless RFID technology, that bridges the technological gap to some extent among the classic RFID with chip, is electronic rewritability. We have reported recently a handful of studies in which an emerging non-volatile RF switching technology known as CBRAM (Conductive Bridging Random Access Memory) is utilized for the realization of electronically rewritable chipless RFID tags [8], [9]. CBRAM is an efficient and non-volatile RF switching solution suitable for electronically rewritable chipless RFID applications due to its low cost and simplicity in terms of fabrication [9], [10].

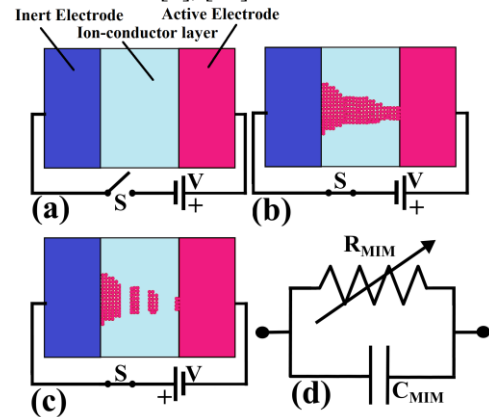


Figure 1. Layer structure and working principle of CBRAM switches. (a) CBRAM cell structure. (b) Set (ON) process leading to low resistance state (LRS). (c) Reset (OFF) process leading to high resistance state (HRS). (d) Electrical equivalent model.

Figure 1 shows the layer architecture of a CBRAM switch, which operates with the principle of electrochemical growth of a metallic filament among an electrochemically opposite electrode pair (aluminum and copper or silver and aluminum) sandwiching a suitable ion-conductor among them. Introduction of the utilization of polymer ion-conductors like Nafion in CBRAM RF switching applications has added so much to the versatility and fabrication simplicity of this technology.

We have recently reported the utilization of an emerging AM technique known as thermal impression transfer printing for the realization of electronically rewritable REPs along with the integrated CBRAM switches for chipless RFID applications [11]. Thermal transfer printing of metallic layers is a recent innovation in which a set of micro-machined and computer controlled heated pixel shaped pistons are used to selectively transfer a metallic film from a ribbon former to a suitable substrate of choice as shown in Figure 2. Moreover this is a process compatible with an industrial roll-to-roll process, as shown in Figure 2, promising low cost and high speed fabrication possibilities.

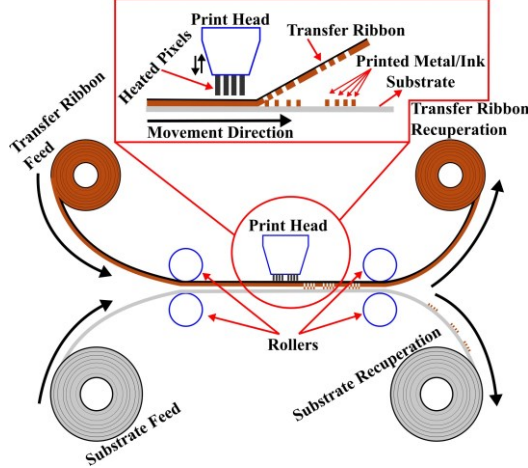


Figure 2. Thermal impression transfer printing process.

In this article we present the design and realization of an electronically rewritable REP for chipless RFID applications on flexible PET substrate fabricated using thermal transfer printing process. This REP encodes the most number of bits among electronically rewritable REPs reported till date.

2 Design

In this section we present design and simulation results of the proposed electronically rewritable resonator for chipless RFID applications. This REP is inspired from the C-shaped rewritable resonator reported in [8]. Here instead of one, we add two CBRAM switches in the resonator geometry by adapting the trace widths as shown in Figure 3.

The two CBRAM switches are formed each between the traces marked as 'W1' and 'W2' by interposing a 600 nm layer of Nafion (ion-conductor), as shown in Figure 3. The design is initially simulated in CST Microwave Studio in full wave electromagnetic simulation mode, in which the CBRAM cells are modeled as their respective electrical models, (as shown in Figure 1), to speed-up the process. The parameter values of the electrical model are calculated directly from the geometry of the CBRAM switch design, and are optimized through knowledge of the electrical model behavior from previous studies [10], [11]. In this design the electrical length of the resonator is electronically tuned, forcing it to resonate at four different resonance frequencies depending on the ON or OFF states

of the integrated CBRAM switches. The simulated RCS backscatter response of this resonator is depicted in Figure 4. Here the CBRAM switch is modeled to have a low resistance state (LRS) of $1 - 10 \Omega$ in its ON state and a high resistance state (HRS) of $1 \text{ M}\Omega$ in its OFF state. The equivalent OFF state capacitance of the CBRAM switch is modeled to be around 1.16 pF .

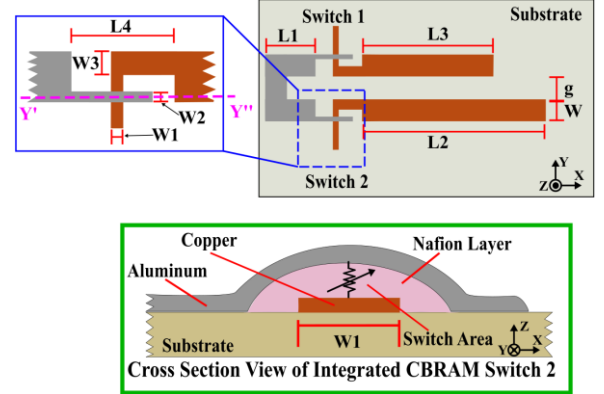


Figure 3. Geometry of proposed electronically rewritable resonator (REP) for chipless RFID applications. $L1 = 7.5 \text{ mm}$, $L2 = 27.5 \text{ mm}$, $L3 = 22.5 \text{ mm}$, $L4 = 3 \text{ mm}$, $W = 3 \text{ mm}$, $W1 = W2 = 0.15 \text{ mm}$, $w3 = 1.5 \text{ mm}$, $g = 3 \text{ mm}$. (Layer thickness: Aluminium = 200 nm , Copper = 300 nm , Nafion = 600 nm , PET substrate = $100 \mu\text{m}$).

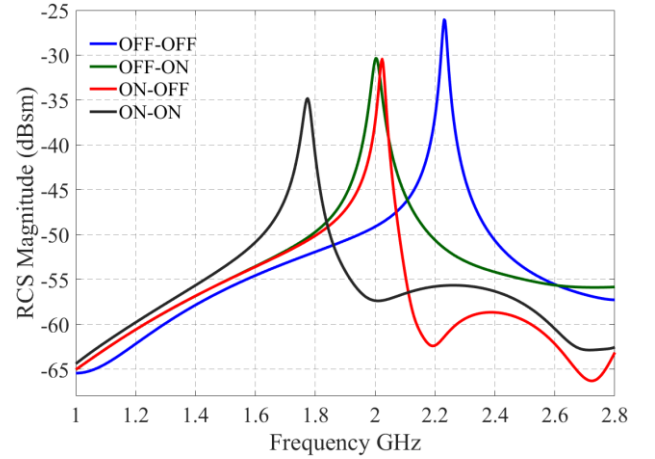


Figure 4. Simulated (full wave) RCS backscatter response of electronically rewritable resonator (REP) depicted in Figure 3, for all possible combinations of integrated CBRAM switches.

3 Fabrication, Results and Discussions

The presented design of electronically rewritable resonator is realized through thermal transfer printing technique using the Zebra ZT610 printer. Figure 5 shows the photograph of the realized electronically rewritable REP, on flexible PET substrate. The fabrication process is carried out in three steps. Initially, one of the metallic layers (aluminum or copper) is printed on the PET substrate. Then reference for the next print in manually marked and the ion-conductor layer is formed by spin coating of nafion impregnated resin solution [11] and is

allowed to dry. Later the substrate is loaded back to the printer and the next metallic layer (opposite to the previous layer – say copper or aluminum respectively) is printed to complete the realization process. The thicknesses of the printed metal layers are measured to be around 200 to 300 nm. The printed layers show a sheet resistivity of 0.5050 $\Omega/\text{sq.}$ and 0.3790 $\Omega/\text{sq.}$ respectively for aluminum and copper.

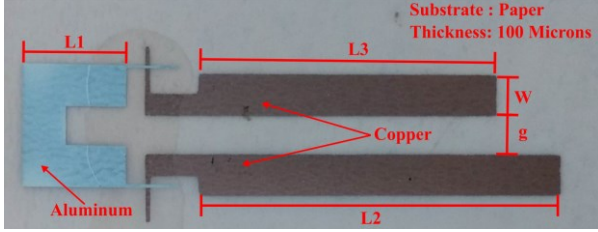


Figure 5. Photograph of fabricated electronically rewritable chipless RFID tag with one REP, on flexible PET substrate. $L1 = 7.5$ mm, $L2 = 27.5$ mm, $L3 = 22.5$ mm, $W = 3$ mm, $g = 3$ mm.

The realized electronically rewritable resonator for chipless RFID applications is measured using a bi-static RCS reader setup, arranged in a semi-anechoic chamber, wired around a Keysight N5222A Network Analyzer and two open boundary quad ridged horn antennas in co-polarization to each other, and to the tag (along the Y axis shown in Figure 3), and is depicted in Figure 6.

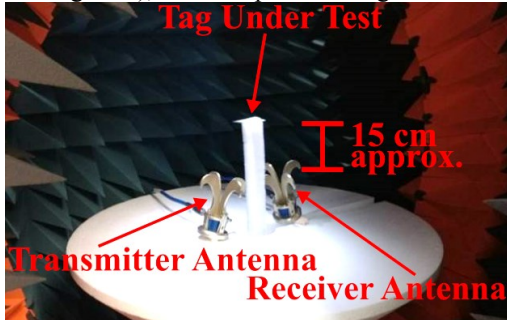


Figure 6. Photograph of bistatic experimental setup used to capture the RCS backscatter response of chipless RFID tags. Distance between tag and antenna tip: ~ 15 cm.

Integrated CBRAM switches in the realized electronically rewritable REP is operated using optimized DC pulses applied directly through the metallic parts of the tag, using simple electrical clamps [10]. The measured RCS backscatter response (uncalibrated) of the electronically rewritable chipless RFID tag with one REP is depicted in Figure 7. One could see from this figure that all the possible four states of this resonator is clearly distinguishable and readable, thus proving the feasibility of such an approach. Moreover, the experimentally observed RCS backscatter response is in good agreement with the results of the full wave simulation thus demonstrating the accuracy of the model. The quality factor of the realized design is a bit low in comparison to the simulation and is due to the higher sheet resistivity of printed metal layers. An RCS level similar to as observed in the full wave simulation results are expected for the

realized tag and the complete characterization of the same is in rapid progress with the authors.

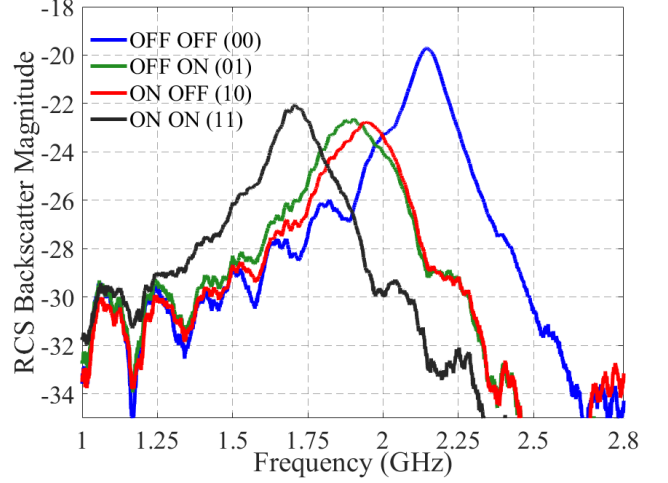


Figure 7. Experimentally obtained RCS backscatter (uncalibrated) response of electronically rewritable chipless RFID tag depicted in Figure 5, for all possible combinations of integrated CBRAM switches. CBRAM ON state (LRS): 1 - 10 Ω , OFF state (HRS): 100 k Ω - 1 M Ω

4 Future Perspectives

A total of five to six REPs proposed herewith could be arranged on to a standard credit card sized tag. As such a coding capacity of 10 to 12 bits could be attained through the presented approach. Further design optimizations and characterizations in these directions are in rapid progress with the authors and are expected to be reported in open literature in near future.

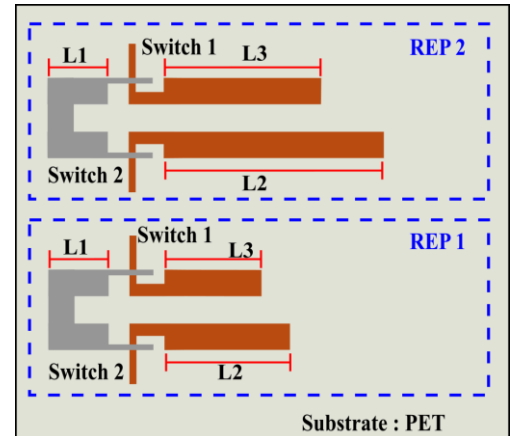


Figure 8. Layout of electronically rewritable chipless RFID tag with two REPs of the proposed kind. (All dimensions similar to as shown in Figure 3, except, $W1 = W2 = 0.1$ mm, REP1: $L2 = 27.5$ mm and $L3 = 22.5$ mm, REP2: $L2 = 17.5$ mm and $L3 = 10.5$ mm.)

Towards these directions, in this section, we present the full-wave simulation results of an electronically rewritable chipless RFID tag with two such REPs. Figure 8 shows the layout and geometry of this design and Table I summarizes the resonance states for all possible

combinations of integrated CBRAM switches in this tag (16 states – 4 bits). Figure 9 shows the simulated (full wave) RCS backscatter response of some selected states for immediate information to the readers about the selectivity and RCS magnitude level of the response. All the states summarized on Table I follow this trend.

Table I. Frequency of resonance observed in simulated (full wave) RCS backscatter response of electronically rewritable chipless RFID tag shown in Figure 8.

Code	REP1		REP2		RCS Backscatter Response	
	R1	R2	R3	R4	F1 (GHz)	F2 (GHz)
1111	OFF	OFF	OFF	OFF	2.8456	3.3800
1110	ON	OFF	OFF	OFF	2.7017	2.8456
1101	OFF	ON	OFF	OFF	2.8456	2.992
1100	ON	ON	OFF	OFF	2.3424	2.8456
1011	OFF	OFF	OFF	ON	2.2911	3.4218
1010	ON	OFF	OFF	ON	2.2911	2.7272
1001	OFF	ON	OFF	ON	2.2911	2.9996
1000	ON	ON	OFF	ON	2.2911	2.3699
0111	OFF	OFF	ON	OFF	2.1933	3.3673
0110	ON	OFF	ON	OFF	2.1933	2.7143
0101	OFF	ON	ON	OFF	2.1933	2.9873
0100	ON	ON	ON	OFF	2.1933	2.3584
0011	OFF	OFF	ON	ON	1.7043	3.4512
0010	ON	OFF	ON	ON	1.7043	2.6891
0001	OFF	ON	ON	ON	1.7043	2.9895
0000	ON	ON	ON	ON	1.7043	2.3400

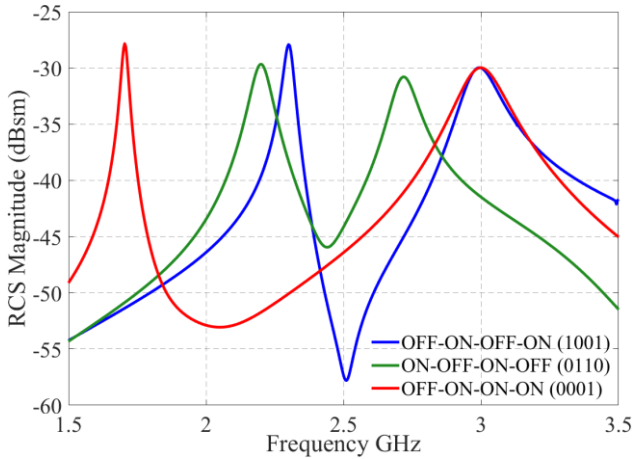


Figure 9. Simulated (full wave) RCS backscatter response of electronically rewritable chipless RFID tag shown in Figure 8, for some selected combinations of integrated CBRAM switches.

5 Conclusion

We have affirmatively presented the design, realization and future perspectives of an electronically rewritable REP for chipless RFID applications on PET substrate, with a coding capacity of 2 bits per REP and realized through an AM based printing process. Further designs expansions, investigation on mitigation of present drawbacks, and detailed characterization of the presented approach and devices are in rapid progress with the authors and are expected to be published soon in open literature.

6 Acknowledgements

This project has received funding from the European Research Council (ERC) under European Union's Horizon 2020 research and innovation program (grant agreement No 772539, ScattererID project). <https://www.scattererid.eu/>.

7 References

- [1] S. Tedjini, N. Karmakar, E. Perret, A. Vena, R. Koswatta, and R. E-Azim, "Hold the Chips: Chipless Technology, an Alternative Technique for RFID," *IEEE Microw. Mag.*, vol. 14, no. 5, pp. 56–65, Jul. 2013, doi: 10.1109/MMM.2013.2259393.
- [2] F. Costa *et al.*, "Progress in green chipless RFID sensors," in *2017 11th European Conference on Antennas and Propagation (EUCAP)*, Mar. 2017, doi: 10.23919/EuCAP.2017.7928460.
- [3] E. Perret, *Radio Frequency Identification and Sensors: From RFID to Chipless RFID*. Hoboken, NJ, USA: Wiley, 2014.
- [4] A. Vena, E. Perret, and S. Tedjini, *Chipless RFID based on RF Encoding Particle: Realization, Coding and Reading System*. New York, NY, USA: ISTE Press - Elsevier, 2016.
- [5] M. Garbati, E. Perret, R. Siragusa, and C. Halope, "Ultrawideband Chipless RFID: Reader Technology From SFCW to IR-UWB," *IEEE Microw. Mag.*, vol. 20, no. 6, pp. 74–88, Jun. 2019, doi: 10.1109/MMM.2019.2904408.
- [6] Marco Garbati, Etienne Perret, Romain Siragusa, *Chipless RFID Reader Design for Ultra-Wideband Technology - 1st Edition*, 1st ed. ISTE Press - Elsevier, 2018.
- [7] A. Attaran and R. Rashidzadeh, "Chipless Radio Frequency Identification Tag for IoT Applications," *IEEE Internet Things J.*, vol. 3, no. 6, pp. 1310–1318, Dec. 2016, doi: 10.1109/JIOT.2016.2589928.
- [8] J. M.P., A. Vena, B. Sorli, and E. Perret, "Solid-State Conductive-Bridging Reconfigurable RF-Encoding Particle for Chipless RFID Applications," *IEEE Microw. Wirel. Compon. Lett.*, vol. 28, no. 6, Jun. 2018, doi: 10.1109/LMWC.2018.2830702.
- [9] J. Methapettyparambu Purushothama, E. Perret, and A. Vena, *Non Volatile CBRAM/MIM Switching Technology for Electronically Reconfigurable Passive Microwave Devices*. NY, USA: ISTE Press – Elsevier - Accepted for publication, 2020.
- [10] M. P. Jayakrishnan, A. Vena, A. Meghit, B. Sorli, and E. Perret, "Nafion-Based Fully Passive Solid-State Conductive Bridging RF Switch," *IEEE Microw. Wirel. Compon. Lett.*, vol. 27, no. 12, Dec. 2017, doi: 10.1109/LMWC.2017.2764741.
- [11] J. M. P., S. Lopez-Soriano, A. Vena, I. Susanti, B. Sorli, and E. Perret, "Electronically Rewritable Chipless RFID Tags Fabricated Through Thermal Transfer Printing on Flexible PET Substrates," *IEEE Trans. Antennas Propag.*, Oct. 2020, doi: <https://doi.org/10.1109/TAP.2020.3030965>.